Journal of Medicinal Chemistry

Article

pubs.acs.org/jmc

Identification of Selective Inhibitors for Human Neuraminidase Isoenzymes Using C4,C7-Modified 2-Deoxy-2,3-didehydro-*N*-acetylneuraminic Acid (DANA) Analogues

Yi Zhang,[†] Amgad Albohy,[†] Yao Zou,[†] Victoria Smutova,[‡,§] Alexey V. Pshezhetsky,[‡,§] and Christopher W. Cairo*[,†]

[†]Alberta Glycomics Center, Department of Chemistry, University of Alberta, Edmonton, Alberta T6G 2G2, Canada

[‡]Division of Medical Genetics, Centre Hospitalière Universitaire Sainte-Justine, University of Montreal, Montreal, Quebec, Canada

[§]Department of Anatomy, Cell Biology, Faculty of Medicine, McGill University, Montreal, Quebec, Canada

Supporting Information

ABSTRACT: In the past two decades, human neuraminidases (human sialidases, hNEUs) have been found to be involved in numerous pathways in biology. The development of selective and potent inhibitors of these enzymes will provide critical tools for glycobiology, help to avoid undesired side effects of antivirals, and may reveal new small-molecule therapeutic targets for human cancers. However, because of the high active site homology of the hNEU isoenzymes, little progress in the design and synthesis of selective inhibitors has been realized. Guided by our previous studies of human NEU3 inhibitors, we designed a series of C4,C7-modified analogues of 2-deoxy-2,3-didehydro-*N*-acetylneuraminic acid (DANA) and tested them against the full panel of hNEU isoenzymes (NEU1, NEU2, NEU3, NEU4). We identified inhibitors with up to 38-fold selectivity for NEU3 and 12-fold selectivity for NEU2 over all other isoenzymes. We also identified compounds that targeted NEU2 and NEU3 with similar potency.

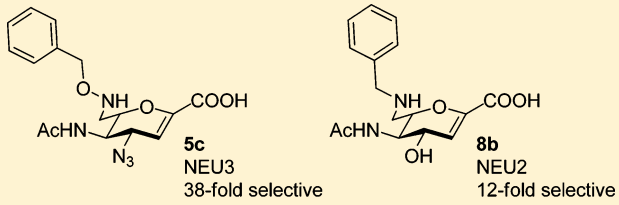

INTRODUCTION

The glycosylation of proteins can alter cell signaling, protein−ligand and protein−protein interactions, and protein stability.[1−3] Most of glycan biosynthesis occurs in the endoplasmic reticulum and Golgi compartments of the cell.[1] However, enzymatic modification of glycan structures also occurs after glycoprotein biosynthesis, a process known as glycan remodeling. The effects of this process can be seen in measures of the relative half-life of glycan structures versus the protein backbone.[4,5] Glycan remodeling is gaining recognition as an important regulatory function within mammalian cells.[6] While glycan remodeling is implicated in cell signaling,[7] there remains a lack of chemical tools to probe the specific enzymes that participate in these processes. Two likely instigators of this process are glycosyl hydrolase (GH) and glycosyl transferase (GT) enzyme classes, which degrade and synthesize the glycosidic linkage, respectively. Thus, strategies for chemical inhibition of mammalian GH and GT are of interest for exploring cell signaling pathways.[8] The challenge, however, is to design potent inhibitors with selectivity for specific isoenzymes within each class in order to avoid potentially toxic effects.

Membrane-associated GH regulate signaling pathways through cleavage of glycolipids and glycoproteins. A number of membrane-associated glycosidases are known in mammalian cells including β-galactosidase,[9] β-glucosidase,[10] α- and β-mannosidase,[11] α-fucosidase,[12] and four isoenzymes of neuraminidase (also known as sialidase).[13] Among these enzymes, the neuraminidase enzymes (NEU1, NEU2, NEU3, and NEU4) have been shown to participate in a variety of signaling pathways and pathologies including inflammation,[14,15] adhesion,[7,16] tumorigenesis,[17] and cancer metastasis.[18,19] Notably, sialic acid content in cells and serum is altered in autoimmune diseases; for example, multiple sclerosis patients have decreased levels of sialic acid on their cell membranes[20] and increased free sialic acid in serum.[21] These and other examples support the hypothesis that hNEUs are important regulators in health and disease, and are therefore potential therapeutic targets. Yet there are few examples of specific inhibitors for this family of enzymes.

The design of specific chemical inhibitors for hNEU must take into account the similarities between isoenzymes. The four hNEU enzymes are classified as family 33 GH[22] and *exo*-sialidases (EC 3.2.1.18).[23] They vary in their subcellular location and substrate specificity. NEU1 is localized at the lysosomal and plasma membranes.[24,25] NEU2 is a soluble protein found in the cytosol.[26−28] NEU3 is a membrane-associated protein localized in the caveolae microdomains of plasma membranes,[29] as well as endosomal and lysosomal membranes.[30] The *NEU4* gene can be differentially spliced, resulting in the appearance of two NEU4 isoforms that differ in the first 12 N-terminal amino acids.[31,32] The short isoform of

Received: December 22, 2012
Published: March 26, 2013

NEU4 is found predominantly on the ER membranes,[31,32] whereas the long form is targeted to both mitochondria[31,32] and lysosomes.[33] Genetic defects in NEU1 result in autosomal pediatric sialidosis disease associated with lysosomal storage of sialylated glycopeptides and oligosaccharides.[34] NEU3 is selective for glycolipids over glycoproteins[33] and has been reported to be modulated by signaling events such as protein kinase C activation in immune cells.[35]

Only a few investigations have explored the substrate specificity of hNEU beyond native glycolipids,[36,37] providing limited data for the design of synthetic substrates or inhibitors. Inhibitor selectivity for human NEU2 over bacterial enzymes has been investigated and seems to suggest that these two enzymes have significantly different preferences.[37,38] Magesh et al. have reported compounds that selectively target NEU1 with micromolar activity.[39] However, inhibitors that target NEU2, NEU3, and NEU4 enzymes remain to be identified.

We set out to generate a small panel of 2-deoxy-2,3-didehydro-*N*-acetylneuraminic acid (DANA) analogues that contained modified C7 side chains. Previous reports have suggested that a basic functional group at the C4 position may increase inhibitory activity.[40] Therefore, C4-modified compounds were included in our scheme to probe the combination of these two strategies (Scheme 1). Upon testing of these DANA derivatives against the four human neuraminidase isoenzymes, as well as a bacterial isoenzyme (*Vibrio cholera* neuraminidase, *vc*NEU), we confirmed that NEU2 and NEU3 tolerate large hydrophobic groups at the C7 position. Importantly, we found that modification of the DANA scaffold at the C7 side chain can impart selectivity for inhibitors among members of the hNEU family. We identified a NEU3 inhibitor with nearly 40-fold selectivity over other isoenzymes (**5c**) and a NEU2 inhibitor with 12-fold selectivity (**8b**). We propose that these results can be used to accelerate the identification of more potent and isoenzyme-selective hNEU inhibitors.

Scheme 1. Inhibitor Targets

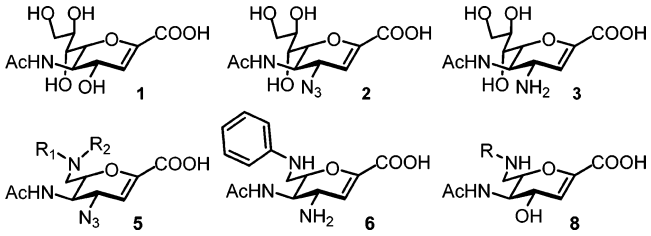

RESULTS

Inhibitor Synthesis. We set out to synthesize DANA (**1**) analogues containing C4 and C7 modifications individually or in combination (Scheme 1). To introduce an azide at C4, we employed established methods via nucleophilic opening of an oxazoline intermediate, producing compound **2** after deprotection.[41,42] Subsequent reduction of the azide to an amine provided compound **3**. Modification at C7 was accomplished via oxidative cleavage at C7−C8 using sodium periodate.[43] The resulting aldehyde could then be used for a variety of coupling chemistries including reductive amination and oxime or hydrazide formation. DANA analogues containing a C4-azide were generated by coupling to **4** (Scheme 2),[44−46] while analogues with the C4-hydroxyl were generated by coupling to **7** (Scheme 3).[43] Reductive coupling of aldehyde **4** was performed with several nucleophiles, including aromatic amines (**5a**, **5b**), phenylhydrazine (**5e**), and benzylic hydroxylamines (**5c**, **5d**). Reduction of the C4-azide of compound **5a** with Lindlar's catalyst afforded the corresponding amine **6**. Although we expected that the oxime linkage initially formed in the coupling of **5c** would be stable, we chose to reduce the oxime to avoid the formation of diastereomers.[47] Coupling of compound **7** followed an identical protocol to compound **4** using aniline (**8a**), benzylamine (**8b**), and biphenylmethylhydrazine (**8c**) nucleophiles.

Inhibition Assays. To determine the potency of DANA analogues against separate isoenzymes of hNEU, enzyme samples were produced either by recombinant expression or by purification from human cells. NEU1 was purified as a protein complex with β-galactosidase and cathepsin A, following previous protocols.[48] Human NEU2,[49] NEU3,[50]

Scheme 2. Synthesis of C4- and C4,C7-Subsituted DANA Derivatives

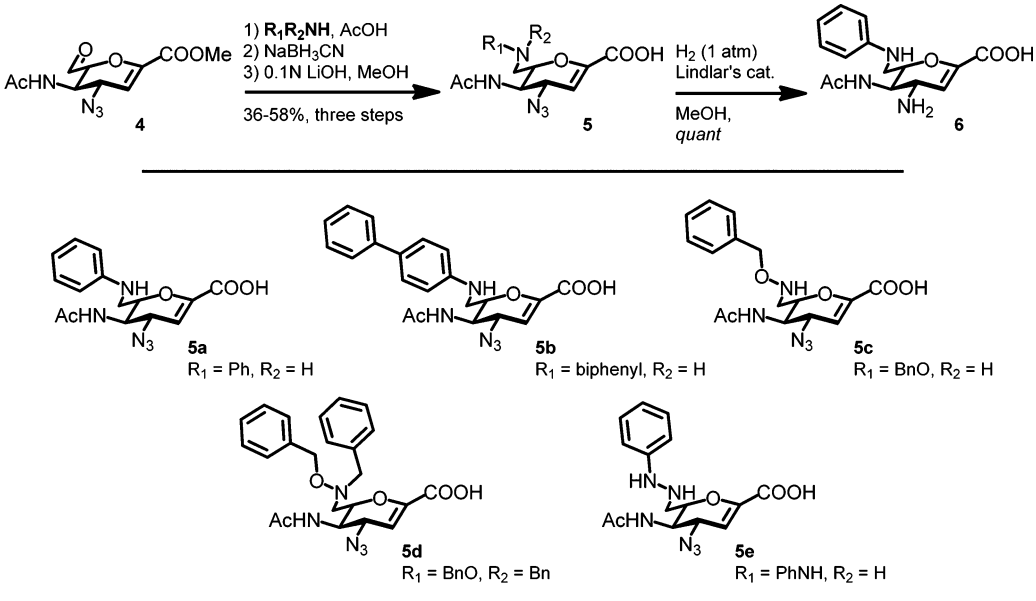

dx.doi.org/10.1021/jm301892f | J. Med. Chem. 2013, 56, 2948−2958

Scheme 3. Synthesis of C7-Substituted DANA Derivatives

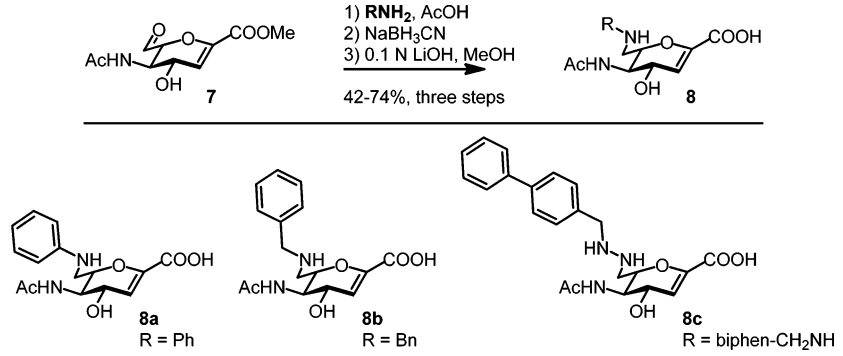

Table 1. Inhibition of Neuraminidase Isoenzymes

			IC_{50} (μM)[a]									
Compound	Relative activity[b]		NEU1		NEU2		NEU3		NEU4		*V.c.* sialidase	
	Target	Selectivity	IC_{50}	±	IC_{50}	±	IC_{50}	±	IC_{50}	±	IC_{50}	±
DANA (1)	hNEU	4	80	10	90	10	6.3	0.5	13	1	170	30
2	NEU2,3	7	360	50	59	13	54	5	1000	60	540	60
3	NEU2	4	> 1000	-	44	3	180	20	720	70	> 1000	-
5a	NEU2	2	> 1000	-	131	31	440	300	300	20	> 1000	-
5b	NEU2, 3	3	> 1000	-	74	4	50	30	210	10	> 1000	-
5c	NEU3	38	> 1000	-	920	200	24	2	> 1000	-	550	70
5d	NEU3	7	> 1000	-	173	50	24	11	350	180	> 1000	-
5e	NEU2,3	33	> 1000	-	40	7	20	8	> 1000	-	> 1000	-
6	NEU3	1.5	> 1000	-	800	30	540	30	>1000	-	> 1000	-
8a	NEU2	4	> 1000	-	100	13	370	80	> 1000	-	> 1000	-
8b	NEU2	12	> 1000	-	86	17	> 1000	-	> 1000	-	470	80
8c	NEU2,3	3	> 1000	-	67	18	70	20	200	20	> 1000	-

[a]Coloring of potency values is by relative ranking within each isoenzyme. Darker shades of red indicate higher potency compounds with activity below 500 μM or that are ranked in 1−7 among compounds tested. Darker shades of blue indicate weaker potency, with activities typically above 500 μM or that are ranked 8−12 among compounds tested. [b]Relative activity was determined by dividing the potency of the compound for its next weakest target by that of its primary target. For cases where multiple isoenzymes are listed as the target, the average of these was used.

and NEU4[51] were expressed as fusion proteins following previous reports. With all four human isoenzymes in hand, we first compared the pH profiles of each enzyme using a fluorogenic substrate, 2′-(4-methylumbelliferyl)-α-D-*N*-acetylneuraminic acid (4MU-NANA). All four enzymes had optimal enzymatic activity in acidic environments. NEU1, NEU3, and NEU4 showed narrow activity ranges between pH 4 and pH 5. In contrast, NEU2 gave a wide range of activity between pH 5 and pH 6. We then tested the potency of DANA against each enzyme using the 4MU-NANA substrate. We found that DANA was indeed a general and nonselective inhibitor with low micromolar (6−90 μM) activity against hNEU (Table 1). For comparison, we tested the activity of DANA against a bacterial enzyme, *vc*NEU. DANA was at least 4-fold more potent against all members of the hNEU family, relative to *vc*NEU. The inhibition constants (K_i) of DANA against three of the human isoenzymes were determined for comparison (NEU2, 5 ± 2 μM; NEU3, 2.2 ± 0.5 μM; NEU4, 1.0 ± 0.6 μM).

Testing of the remaining compounds revealed that in comparison to DANA (**1**), modification of the C4 substituent from a hydroxyl to a bulkier azide (**2**) reduced potency against NEU1 and NEU4. This effect was most pronounced in the case of NEU1 for the *C*4-amino derivative **3**. Interestingly, NEU2 was the most tolerant of C4 modifications; compound **3** was 2-fold more potent than **1** against NEU2 and showed 4-fold selectivity over other isoenzymes. These results suggested that modifications to the C4 position could be used to gain inhibitor selectivity for NEU2 and NEU3 over other isoenzymes.

The activity of compounds with C4,C7-modifications confirmed that these changes could impart NEU2 and NEU3 selectivity to DANA analogues. Comparison of the activity of compounds where the glycerol side chain of DANA was replaced with a phenylamine (**5a**, **6**, and **8a**) illustrated that the

dx.doi.org/10.1021/jm301892f | J. Med. Chem. 2013, 56, 2948−2958

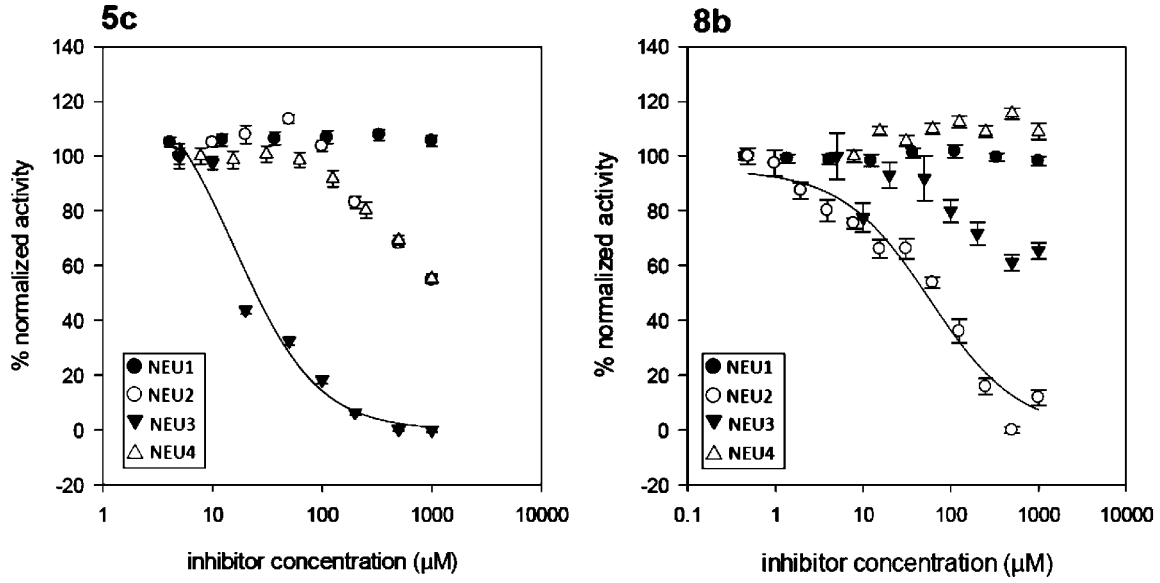

Figure 1. IC_{50} curves of **5c** and **8b** for the four human neuraminidase isoenzymes. The experiments were performed as described in the Experimental Section. **5c** was 38 times more selective for NEU3, and **8b** was 12 times more selective for NEU2 over the other hNEU.

C4-azido, -amino, and -hydroxy groups cannot always compensate for significant modifications at the C7 position. All three compounds had significantly reduced potency in comparison to DANA. Taken together with the results above for compounds **1**–**3**, we concluded that the *C*7-aniline was not able to gain significant contacts in the binding pocket, thus masking any apparent gains from modification at C4. Extension of the C7 group to a phenylhydrazide (**5e**) resulted in a remarkable gain in potency for NEU2 and NEU3. Presumably, the addition of a H-bond acceptor/donor site was partly responsible for the observed 33-fold selectivity for NEU2 and NEU3 over other isoenzymes. Modification of the C7-site to a hydroxyamino group ablated one H-bond donor site from the side chain (**5c**). We observed that **5c** was remarkably selective for the NEU3 isoenzyme (24 ± 2 μM, 38-fold selective) over all other enzymes tested. To the best of our knowledge, this compound is the first confirmed NEU3-specific inhibitor reported.

Examination of the potency data for **8b** and **5c** reveal a dramatic switch in selectivity from NEU2 to NEU3 (Figure 1). Compounds **8b** and **5c** differ in the C4 substituent and the composition of the C7 moiety. Although the addition of a *C*4-amino group improved potency for compound **3** against NEU2, compound **5c** had negligible activity against the enzyme. In contrast, the *C*4-hydroxy-*C*7-benzylamino analogue (**8b**) was 12-fold selective for NEU2. The apparent switch of selectivity between NEU2 and NEU3 is, therefore, not strictly tied to either the C4 or C7 substituents. Chavas et al. have previously observed that, at least in NEU2, the recognition of substrate is dynamic and requires significant rearrangement of the active site.[52] Even so, we were surprised to find that additional steric bulk in the form of an *N*-benzyl group on **5d** did not disrupt NEU3 activity. Instead, this modification reduced NEU3 selectivity (7-fold selective) while improving activity against NEU2.

Next we examined the effect of a large aromatic group at the C7 position. In our previous studies of NEU3, we observed that large hydrophobic groups could be tolerated at the C9 position of DANA.[53] We wanted to determine if the loss of the glycerol side chain could be compensated by incorporation of a hydrazide group. The *C*4-azido-*C*7-biphenylamino analogue **5b** targeted both NEU2 and NEU3 with mid-micromolar activity. The mild selectivity of **5b** was similar to that of the *C*4-hydroxy-*C*7-biphenylmethylamino analogue **8c**. Both **5b** and **8c** had approximately 3-fold selectivity for NEU2 and NEU3, with only moderate activity for NEU4. Finally, we determined the K_i values for the two most potent compounds identified (with IC_{50} < 25 μM) against their target enzyme, NEU3. We found that **5c** had a K_i of 8 ± 1 μM against NEU3 and that **5e** had similar activity at 11 ± 3 μM (Table 2).

Table 2. K_i Determinations

compd	enzyme	K_i (μM)
DANA (**1**)	NEU2	5 ± 2
DANA (**1**)	NEU3	2.2 ± 0.5
DANA (**1**)	NEU4	1.0 ± 0.6
5c	NEU3	8 ± 1
5e	NEU3	11 ± 3

Molecular Modeling. We used molecular modeling to gain insight into the selectivity switch of **5c** and **8b** between the NEU3 and NEU2 active sites. We used the structural data reported by Chavas et al. to model ligand interactions with NEU2 (PDB code 1VCU).[52] As no X-ray structure is currently available for NEU3, we employed a homology model of the enzyme that was previously developed in our group.[50] To provide a model of protein–ligand interactions, we performed molecular docking using Autodock 4.2,[54,55] followed by an unrestrained 10 ns molecular dynamics simulation. We evaluated the binding of **5c** with NEU3 and of **8b** with NEU2 using this strategy.

The binding model of **5c** supported our hypothesis that the NEU3 active site can accommodate large hydrophobic groups (Figure 2). The model maintained key contacts between the *C*1-carboxylate and the arginine triad, as well as those of the *N*5-Ac pocket. The *C*4-azido group was well accommodated by the O4 pocket (I26, D50, M87, and N88). The C7 side chain of **5c** contains a four-atom linker to the phenyl group and contains two H-bond acceptors and one H-bond donor. The distance

dx.doi.org/10.1021/jm301892f | J. Med. Chem. 2013, 56, 2948–2958

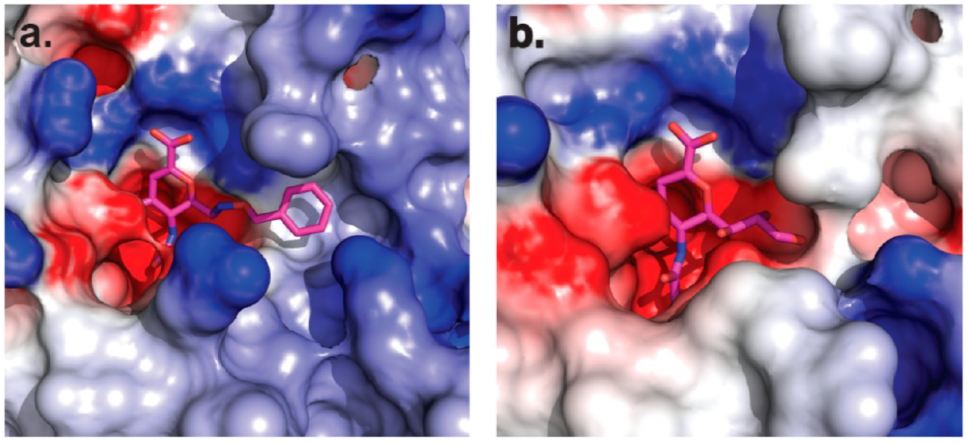

Figure 2. Molecular models of the NEU2 and NEU3 active sites. (a) A model of the protein−ligand complex was generated using docking and molecular dynamics (see Experimental Section). The large hydrophobic pocket of NEU3 accommodates the C7 side chain of compound **5c**. (b) The active site topology of NEU2 (PDB code 1VCU)[52] is shown for comparison and reveals a smaller pocket for the glycerol side chain of DANA (C7−C9). Electrostatic potential surfaces were generated with DelPhi[63] and visualized using PyMOL.[62]

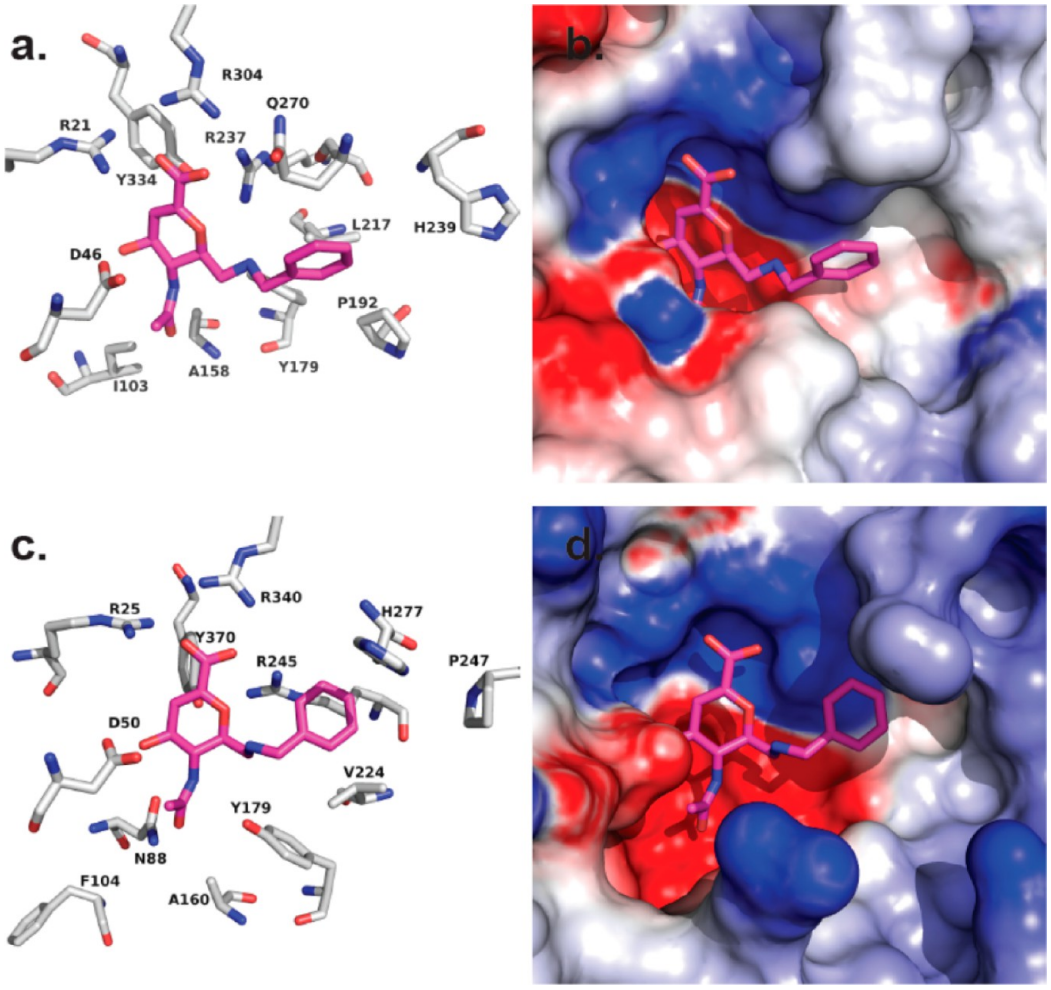

Figure 3. (a) A molecular model of compound **8b** bound to NEU2 postulates a binding mode with the phenyl group interacting with the hydrophobic portion of Q270 and interacting with L217 and P192. (b) The electrostatic potential surface of NEU2 shows that the region interacting with the phenyl ring is relatively nonpolar. (c) A molecular model of **8b** in the active site of NEU3 shows that while the C7 side chain can be accommodated sterically, the linker positions the phenyl ring in a region of the binding pocket where it cannot gain any significant contacts. (d) An electrostatic potential surface of NEU3 reveals that the phenyl ring of **8b** is positioned in a relatively polar region of the binding pocket.

between the pyranoside ring and the phenyl group would not allow for interactions with H277 (the groups are ∼5−6 Å apart). However, the phenyl group could gain hydrophobic interactions with several residues of the active site (V224, V222, P247, P198). An inspection of the NEU2 active site revealed that the side chain of **5c**, were it in the same conformation as

dx.doi.org/10.1021/jm301892f | *J. Med. Chem.* 2013, 56, 2948−2958

predicted for NEU3, would result in a steric clash with Q270. We propose that this difference between the active site topology results in the selectivity observed for inhibitors with larger C7 groups. Additionally, the model predicts that a shorter C7 group would be better accommodated in the NEU2 active site.

We next examined the selective binding of **8b** to the NEU2 active site (Figure 3). The model of **8b** maintained the same contacts to the active site for the C1-carboxylate, O4, and *N*5Ac groups as observed with DANA and NEU2. The C7 side chain was the only point of departure from DANA. In this case the C7 side chain contained a phenyl group; however, the linker between the pyranoside ring and the arene has been truncated to three atoms and contains only one H-bond donor and acceptor. In this binding mode, the linker could gain a H-bond contact with Y181 (3.4 Å) and hydrophobic interaction with L217 and Q270(C_β). Thus, the relatively small C7 side chain, with its shorter linker, packs into the restricted space available in the NEU2 pocket and gains contacts that improve its activity for the enzyme. In contrast, the NEU3 pocket is too large for effective packing of the **8b** side chain, resulting in a loss of one H-bond contact and leaving the phenyl ring more solvent exposed. The C7 side chain of **8b** positions the phenyl group near relatively polar residues (H277, Y181, and R245), where it is unable to contact the hydrophobic groups that benefit **5c** binding in the NEU3 pocket.

DISCUSSION

In this study we have found that modification of the DANA inhibitor scaffold at the C4 and C7 positions resulted in compounds with improved specificity against the hNEU isoenzymes NEU2 and NEU3. Importantly, we identified lead compounds with 38-fold (**5c**) and 12-fold (**8b**) selectivity for these two isoenzymes, respectively. These are the first reported compounds that have been confirmed to be selective for NEU2 and NEU3 over other hNEUs. While our data confirmed that DANA (**1**) was a nonselective inhibitor of hNEU, we also identified compounds that could target a subset of hNEU isoenzymes. For example, compounds **2**, **5b**, **5e**, and **8c** inhibit NEU2 and NEU3 with comparable potency. These compounds provide an important starting point for the future design of more potent and selective compounds targeting individual human neuraminidases.

There are very few reports of isoenzyme-selective hNEU inhibitors, and yet selective small molecule inhibitors are needed to expand our understanding of this important family of enzymes. Despite the fact that nanomolar inhibitors of viral sialidases are known,[56] the most potent inhibitors reported for hNEU have inhibitory constants in the low micromolar range.[39,53] Interestingly, nanomolar inhibitors of influenza viral sialidase are significantly less active against hNEU.[51,57] Zanamivir (a *C*4-guanidino-modified DANA analogue) is reported to be the most potent of the viral inhibitors against hNEU, with moderate selectivity for NEU2.[57] We observed that a *C*4-azido analogue of DANA (**2**) had similar selectivity for both NEU2 and NEU3 isoenzymes. Few other reports have tested inhibitors designed to target individual hNEUs among the four isoenzymes. Several compounds selective for NEU1 have been identified.[39] Our group has previously identified oseltamivir analogues that were weakly selective for NEU3 over NEU4.[51] Although other studies have examined the activity of inhibitors against hNEU individually, without data on their activity against other isoenzymes it is difficult to judge their utility in vivo where they will compete against the full battery of hNEUs.[38,53,58]

Known inhibitors of hNEU have primarily been based upon the 2-deoxy-2,3-didehydro-*N*-acetylneuraminic acid (**1**) core. The sequence homology of hNEU enzymes suggests that many recognition elements of the active site are preserved across the family.[59] Although X-ray structural data are only available for NEU2, DANA analogues with fewer H-bond donor groups in place of the glycerol side chain are known to disrupt the H-bond network of the active site and reduce potency against NEU2.[52,58] The recognition of the glycerol side chain of sialic acid by hNEUs involves contacts from multiple tyrosine residues.[50,52,59] This arrangement is in contrast to the viral enzyme and could potentially be exploited to improve inhibitor selectivity.[51] Modifications at the C9 position have yielded NEU1 selective inhibitors.[39] We[53] and others[37,38] have explored *C*9- and *N*5-Ac-modified analogues of DANA and their inhibitory potency against NEU3 and NEU2 isoenzymes, respectively. Modification of DANA by inclusion of a *C*4-guanidino group improved potency against NEU2[58] and NEU3.[57]

Although the best compounds identified here have relatively low potency ($K_i \approx 8-11\ \mu M$) for in vivo studies, they represent the first panel of compounds to selectively target NEU2 and NEU3. The most interesting trends observed are the apparent selectivity switch observed between NEU2 and NEU3. The activity of several compounds suggests similarities between substrate recognition by these two isoenzymes. Compounds **2**, **5b**, **5e**, and **8c** show little distinction between NEU2 and NEU3. In contrast, **5c** and **8b** selectively target NEU3 and NEU2, respectively, with only minor structural differences between the compounds. Molecular modeling suggested that the differences between the recognition of these two active sites can be attributed to the topology of the glycerol side chain binding pocket. The NEU3 binding pocket is more accommodating to larger groups and contains several polar contacts that are distal to the position of the *C*9-hydroxyl of the native substrate. In the case of NEU2, the binding pocket relies on hydrophobic packing with smaller side chains. The NEU2 Q270 residue may act as a gatekeeper that prevents the binding of larger groups in this pocket.

CONCLUSION

On the basis of our results, we conclude that derivatives of the DANA scaffold can act as isoenzyme-selective hNEU inhibitors. Furthermore, the binding pocket for the glycerol side chain (C7−C9 of the sialic acid substrate) is a site of diverse enzyme−substrate interactions that can be exploited to improve the potency and selectivity of inhibitors. The human neuraminidase enzymes are of growing biological interest, and new tools are required to understand their roles in glycobiology. Previously, genetic approaches, such as gene targeting in mice or siRNA, have been used to study the biological roles of human neuraminidase enzymes. However, small molecule inhibitors have inherent advantages because of their rapid onset and reversibility of their effects. Herein, we have described a panel of DANA analogues that achieve selective inhibition of one or multiple hNEU isoenzymes at low micromolar potency. These findings should guide future design of inhibitors with improved potency and selectivity for this family of enzymes. Future work will focus on the development of analogues with improved potency and selectivity, as well as

compounds that can selectively target NEU4, the only remaining isoenzyme with no reported selective inhibitors.

EXPERIMENTAL SECTION

General Synthetic Methods. All reagents, including hydrazines and amines, were purchased from Sigma-Aldrich (Oakville, Ontario, Canada) or Acros Organics unless otherwise noted. Compounds were used without further purification unless otherwise noted. All reactions were carried out under argon at room temperature unless otherwise indicated. Reactions were monitored by analytical TLC on silica gel 60-F_{254} (0.25 mm, Silicycle, Quebec, Canada), and spots were visualized under UV light (254 nm) or stained by charring with ceric ammonium molybdate (CAM). Compounds were purified by flash column chromatography with silica gel (230−400 mesh, Silicycle, Quebec, Canada) or by HPLC. ^{1}H NMR spectra were obtained with a Varian 500, 600, or 700 MHz instrument as noted. ^{13}C NMR spectra were recorded at 125, 150, or 175 MHz. Electrospray ionization mass spectra were recorded on an Agilent Technologies 6220 TOF spectrometer. Target compounds **2** and **3** and intermediate aldehydes **4** and **7** were synthesized according to known protocols.[43−46] Compounds used for inhibitor assays were confirmed to be of ≥95% purity by HPLC (see Supporting Information for details).

General Procedure for Synthesis of 5a−e and 8a−c. To a solution of aldehyde **4** (134 mg, 0.5 mmol) in MeOH (5 mL) was added the appropriate amine or hydrazine (2.5 mmol, 5 equiv) and HOAc (50 μL). The mixture was stirred until TLC (hexane/ethyl acetate, 1:2) showed no starting material remained. Sodium cyanoborohydride (400 mg, 3 mmol) was added and the mixture stirred overnight. The solvent was then concentrated in vacuo. The residue was diluted with ethyl acetate and washed with saturated aqueous $NaHCO_3$ and brine. The organic layer was dried on Na_2SO_4 and concentrated in vacuo. The ester was isolated by flash column chromatography (hexane/ethyl acetate, 1:2). The ester was then hydrolyzed by treatment with 0.1 M LiOH in MeOH (5 mL) for 1 h at room temperature. The product was neutralized with Amberlite IR-120 (H^+ form) followed by filtration and evaporation of the solvent. Yields of **5a−e** ranged from 36% to 58% as noted below.

The synthesis of **8a−c** followed a procedure identical to that for **5a−e**, with the replacement of aldehyde **4** with aldehyde **7** (122 mg, 0.5 mmol). Yields of **8a−c** ranged from 42% to 74% as noted below.

5-Acetamido-2,6-anhydro-3,5-dideoxy-D-*glycero*-D-*galacto*-non-2-enonic Acid (1). ^{1}H NMR (500 MHz, CD_3OD) δ 5.64−5.63 (d, *J* = 2.5 Hz, 1H, H-3), 4.34−4.32 (dd, *J* = 8.5, 2.0 Hz, 1H, H-4), 4.10−4.00 (d, *J* = 1.0 Hz, 1H, H-6), 4.08−3.98 (m, 1H, H-5), 3.89−3.82 (m, 1H, H-8), 3.81−3.78 (dd, *J* = 11.5, 3.0 Hz, 1H, H-9), 3.63−3.60 (m, 1H, H-7), 3.50−3.48 (dd, *J* = 9.5, 1.0 Hz, 1H, H-9), 2.01 (s, 3H, CH_3). ^{13}C NMR (125 MHz, CD_3OD) δ 178.5 ($\underline{C}OCH_3$), 173.2 ($\underline{C}OOH$), 148.8 (C_2), 106.6 (C_3), 75.7 (C_6), 69.8 (C_8), 68.7 (C_9), 67.3 (C_4), 63.5 (C_7), 50.5 (C_5), 22.5 ($CO\underline{C}H_3$). HRMS (ESI) calcd for $C_{11}H_{16}NO_8$ $[M - H]^-$, 290.0881; found, 290.0874.

5-Acetamido-4-azido-2,6-anhydro-3,4,5-trideoxy-D-*glycero*-D-*galacto*-non-2-enonic Acid (2). ^{1}H NMR (500 MHz, D_2O) δ 6.01−6.00 (d, *J* = 1.5 Hz, 1H, H-3), 4.38−4.33 (m, 2H, H-4, H-6), 4.24−4.21 (t, *J* = 8.5 Hz, 1H, H-5), 3.93−3.90 (m, 1H, H-8), 3.87−3.85 (dd, *J* = 10.0, 2.0 Hz, 1H, H-9), 3.67−3.27 (m, 2H, H-7, H-9), 2.06 (s, 3H, CH_3). ^{13}C NMR (125 MHz, D_2O) δ 175.5 ($\underline{C}OCH_3$), 166.4 ($\underline{C}OOH$), 146.4 (C_2), 108.7 (C_3), 76.7 (C_6), 70.8 (C_8), 68.7 (C_9), 63.9 (C_4), 61.1 (C_7), 59.7 (C_5), 23.0 ($CO\underline{C}H_3$). HRMS (ESI) calcd for $C_{11}H_{17}N_2O_7$ $[M - Na]^-$, 289.1041; found, 289.1041.

5-Acetamido-4-amino-2,6-anhydro-3,4,5-trideoxy-D-*glycero*-D-*galacto*-non-2-enonic Acid (3). ^{1}H NMR (500 MHz, D_2O) δ 5.66−5.65 (d, *J* = 2.0 Hz, 1H, H-3), 4.34−4.33 (m, 2H, H-5, H-6), 4.22−4.18 (m, 1H, H-4), 3.98−3.85 (m, 1H, H-8), 3.86−3.84 (m, 1H, H-7), 3.66−3.63 (m, 2H, H-9), 2.06 (s, 3H, CH_3). ^{13}C NMR (125 MHz, D_2O) δ 175.7 ($\underline{C}OCH_3$), 169.4 ($\underline{C}OOH$), 151.6 (C_2), 100.9 (C_3), 76.0 (C_6), 70.6 (C_8), 68.7 (C_9), 64.0 (C_4), 51.1 (C_7), 46.8 (C_5), 22.8 ($CO\underline{C}H_3$). HRMS (ESI) calcd for $C_{11}H_{16}N_4NaO_7$ $[M + Na]^+$, 339.0911; found, 339.0910.

Methyl 5-Acetamido-4-azido-2,6-anhydro-3,4,5-trideoxy-6-formyl-L-*gluco*-hex-2-enonate (4). To a solution of 5-acetamido-2,6-anhydro-4-azido-3,4,5-trideoxy-D-*glycero*-D-*galacto*-non-2-enonic acid methyl ester (119 mg, 0.36 mmol)[44−46] in methanol/water (3:1, v/v, 4 mL) was added sodium periodate (156 mg, 0.729 mmol), and the reaction mixture was stirred at room temperature for 30 min. The precipitate was removed by filtration, and the filtrate was evaporated in vacuo to give a white solid. The aldehyde was typically isolated as a mixture of the aldehyde and the methanolic hemiacetal. ^{1}H NMR (500 MHz, CD_3OD) δ 5.98−5.97 (m, 1H, H-3), 4.71−4.65 (m, 1H, H-7), 4.31−4.15 (m, 2H, H-4, H-5), 4.08−4.03 (m, 1H, H-6), 3.83−3.81 (m, 3H, $COOCH_3$), 1.99−1.98 (d, *J* = 4.5 Hz, 3H, CH_3). ^{13}C NMR (125 MHz, CD_3OD) δ 172.2−171.9 ($\underline{C}OCH_3$), 162.5−162.3 ($\underline{C}OOH$), 144.39−144.38 (C_2), 107.2−106.4 (C_3), 95.0−94.1 (C_7), 78.6−78.4 (C_6), 57.1−56.2 (C_4), 51.7−51.5 ($\underline{C}OOMe$), 48.4−48.2 (C_5), 21.27−21.20 ($CO\underline{C}H_3$). HRMS (ESI) calcd for the methyl hemiacetal sodium adduct, $C_{11}H_{16}N_4NaO_6$ $[M + Na]^+$, 323.0962; found, 323.0959.

5-Acetamido-4-azido-2,6-anhydro-3,4,5-trideoxy-6-((phenylamino)methyl)-L-*gluco*-hex-2-enonic Acid (5a). Compound **5a** was prepared by coupling of compound **4** and aniline following the general procedure given above. The product was obtained in three steps in 36% yield. ^{1}H NMR (600 MHz, CD_3OD) δ 7.37−7.34 (m, 2H, ArH), 7.15−7.09 (m, 3H, ArH), 6.26−6.25 (d, *J* = 5.4 Hz, 1H, H-3), 4.35−4.30 (m, 2H, H-4, H-6), 4.12−4.10 (m, 1H, H-5), 3.63−3.61 (m, 1H, H-7), 3.51−3.49 (m, 1H, H-7), 2.02 (s, 3H, CH_3). ^{13}C NMR (125 MHz, DMSO) δ 174.9 ($\underline{C}OCH_3$), 163.1 ($\underline{C}OOH$), 162.8 (ArC_1), 130.4 (C_2), 129.5 (ArC_3), 122.2 (ArC_2), 117.5 (ArC_4), 106.4 (C_3), 72.4 (C_6), 57.5 (C_4), 49.0 (C_7), 43.9 (C_5), 21.9 ($CO\underline{C}H_3$). HRMS (ESI) calcd for $C_{15}H_{16}N_5O_4$ $[M - H]^-$, 330.1208; found, 330.1218.

5-Acetamido-4-azido-2,6-anhydro-3,4,5-trideoxy-6-(([1,1′-biphenyl]-4-ylamino)methyl)-L-*gluco*-hex-2-enonic Acid (5b). Compound **5b** was prepared by coupling of compound **4** and [1,1′-biphenyl]-4-amine following the general procedure given above. The product was obtained in three steps in 54% yield. ^{1}H NMR (500 MHz, CD_3OD) δ 7.79−7.78 (d, *J* = 7.0 Hz, 2H, ArH), 7.70−7.69 (d, *J* = 6.5 Hz, 2H, ArH), 7.54−7.51 (t, *J* = 6.0 Hz, 2H, ArH), 7.46−7.44 (d, *J* = 7.5 Hz, 3H, ArH), 6.05−6.05 (d, *J* = 4.0 Hz, 1H, H-3), 4.22−4.18 (m, 2H, H-4, H-6), 4.06−4.05 (d, *J* = 4.0 Hz, 1H, H-5), 3.71−3.69 (d, *J* = 6.0 Hz, 2H, H-7), 1.98 (s, 3H, CH_3). ^{13}C NMR (125 MHz, CD_3OD) δ 172.3 ($\underline{C}OCH_3$), 167.7 ($\underline{C}OOH$), 152.2 ($ArC_{1'}$), 147.8 (ArC_1), 141.2 (C_2), 130.1 ($ArC_{3'}$), 128.2 (ArC_3), 127.2 ($ArC_{2'}$), 127.1 ($ArC_{4'}$), 125.6 (ArC_2), 113.2 (ArC_4), 98.4 (C_3), 72.0 (C_6), 55.6 (C_4), 48.4 (C_7), 43.9 (C_5), 20.9 ($CO\underline{C}H_3$). HRMS (ESI) calcd for $C_{21}H_{20}N_5O_4$ $[M - H]^-$, 406.1521; found, 406.1526.

5-Acetamido-4-azido-2,6-anhydro-3,4,5-trideoxy-6-(((benzyloxy)amino)methyl)-L-*gluco*-hex-2-enonic Acid (5c). Compound **5c** was prepared by coupling of compound **4** and *O*-benzylhydroxylamine following the general procedure given above. The product was found to have two rotamers present in an 11:1 ratio as confirmed by analytical HPLC (see Supporting Information). The product was isolated in three steps with 47% yield. ^{1}H NMR (500 MHz, CD_3OD) δ 7.33−7.22 (m, 6H, ArH, NH), 5.70−5.69 (d, *J* = 2.5 Hz, 1H, H-3), 4.65 (s, 2H, CH_2), 4.17−4.08 (m, 2H, H-6, H-4), 3.86−3.83 (dd, *J* = 10.0, 8.5 Hz, 1H, H-5), 3.14−3.11 (dd, *J* = 14.0, 2.0 Hz, 1H, H-7), 2.94−2.90 (dd, *J* = 14.0, 9.5 Hz, 1H, H-7), 1.94 (s, 3H, CH_3). ^{13}C NMR (125 MHz, CD_3OD) δ 172.0 ($\underline{C}OCH_3$), 167.5 ($\underline{C}OOH$), 150.1 (ArC_1), 138.0 (C_2), 128.0 (ArC_3), 127.8 (ArC_2), 127.3 (ArC_4), 101.9 (C_3), 75.1 (C_6), 73.6 ($O\underline{C}H_2Ph$), 58.6 (C_4), 52.1 (C_7), 49.7 (C_5), 21.3 ($CO\underline{C}H_3$). HRMS (ESI) calcd for $C_{16}H_{19}N_5NaO_5$ $[M + Na]^+$, 384.1278; found, 384.1281.

5-Acetamido-4-azido-2,6-anhydro-3,4,5-trideoxy-6-((benzyl(benzyloxy)amino)methyl)-L-*gluco*-hex-2-enonic Acid (5d). Compound **5d** was prepared by coupling of compound **4** and *N*,*O*-dibenzylhydroxylamine[60] following the general procedure given above. The product was obtained in three steps in 52% yield. ^{1}H NMR (600 MHz, D_2O) δ 7.45−7.43 (m, 5H, ArH), 7.35−7.33 (m, 3H, ArH), 7.22−7.20 (m, 2H, ArH), 5.81−5.80 (d, *J* = 3.0 Hz, 1H, H-3), 4.43−4.35 (m, 2H, OCH_2), 4.17−4.14 (dd, *J* = 8.4, 2.4 Hz, 1H, H-4), 4.14−4.11 (d, *J* = 13.2 Hz, 1H, H-6), 4.00−3.97 (t, *J* = 9.0 Hz, 1H, H-5), 3.92−3.87 (m, 2H, NCH_2), 3.12−3.08 (dd, *J* = 13.8, 8.4 Hz, 1H, H-7),

dx.doi.org/10.1021/jm301892f | J. Med. Chem. 2013, 56, 2948−2958

2.91−2.89 (m, 1H, H-7), 1.96 (s, 3H, CH_3). ^{13}C NMR (125 MHz, CD_3OD) δ 171.8 ($\underline{C}OCH_3$), 167.8 ($\underline{C}OOH$), 150.2 (C_2), 139.2 (ArC), 137.1 (ArC), 136.9 (ArC), 129.9 (ArC), 128.7 (ArC), 128.1 (ArC), 128.0 (ArC), 127.8 (ArC), 127.7 (ArC), 127.4 (ArC), 127.0 (ArC), 126.7 (ArC), 100.6 (C_3), 75.4 ($O\underline{C}H_2Ph$), 74.7 (C_6), 63.2 ($N\underline{C}H_2Ph$), 58.2 (C_7), 57.5 (C_4), 52.1 (C_5), 21.3 ($CO\underline{C}H_3$). HRMS (ESI) calcd for $C_{23}H24N_5O_5$ $[M - H]^-$, 450.1783; found, 450.1779.

5-Acetamido-4-azido-2,6-anhydro-3,4,5-trideoxy-6-((2-phenylhydrazinyl)methyl)-L-*gluco*-hex-2-enonic Acid (5e). Compound **5e** was prepared by coupling of compound **4** and phenylhydrazine following the general procedure given above. The product was obtained in three steps and 58% yield. ^1H NMR (500 MHz, CD_3OD) δ 7.19−7.16 (m, 2H, ArH_3), 6.93−6.91 (d, J = 8.5 Hz, 2H, ArH_2), 6.80−6.78 (m, 1H, ArH_4), 5.90−5.89 (d, J = 2.5 Hz, 1H, H-3), 4.24−3.99 (m, 2H, H-4, H-6), 4.00−3.97 (t, J = 9.5 Hz, 1H, H-5), 3.56−3.33 (m, 2H, H-7), 3.28−3.13 (m, 2H, H-7), 1.90 (s, 3H, CH_3). ^{13}C NMR (125 MHz, CD_3OD) δ 173.5 ($\underline{C}OCH_3$), 153.4 ($\underline{C}OOH$), 148.8 (ArC_1), 146.5 (C_2), 129.8 (ArC_3), 121.2 (ArC_2), 115.4 (ArC_4), 106.8 (C_3), 76.9 (C_6), 59.2 (C_4), 50.9 (C_7), 50.7 (C_5), 22.7 ($CO\underline{C}H_3$). HRMS (ESI) calcd for $C_{15}H_{17}N_6O_4$ $[M - H]^-$, 345.1307; found, 345.1317. IR (film) ν 3271, 3061, 2929, 2098, 1712, 1656, 1601, 1555, 1497, 1406, 1375, 1313, 1256, 1148, 1093, 1032, 895, 886, 825, 786, 774, 752, 715, 696, 678, 663 cm^{-1}. $[\alpha]_D^{20}$ 112.96° (*c* 0.55, CH_3OH).

5-Acetamido-4-amino-2,6-anhydro-3,4,5-trideoxy-6-((phenylamino)methyl)-L-*gluco*-hex-2-enonic Acid (6). Acid **5a** (5 mg) was dissolved in MeOH (2 mL) followed by addition of Lindlar's catalyst (5 mg). The system was purged three times with argon, and the resulting mixture was stirred under positive hydrogen pressure at room temperature overnight. The system was purged again with argon, and the reaction mixture was filtered through a plug of Celite. The filtrate was then evaporated under reduced pressure to give the title compound **6** as a white solid (4 mg, quant). ^1H NMR (700 MHz, D_2O) δ 7.54−7.43 (m, 5H, ArH), 6.01−6.00 (d, J = 3.5 Hz, 1H, H-3), 4.67−4.63 (m, 1H, H-6), 4.70−4.52 (t, J = 6.3 Hz, 1H, H-5), 4.22−4.21 (m, 1H, H-4), 3.77−3.72 (m, 2H, H-7), 1.99 (s, 3H, CH_3). ^{13}C NMR (175 MHz, D_2O) δ 174.9 ($\underline{C}OCH_3$), 165.1 ($\underline{C}OOH$), 146.0 (ArC_1), 134.4 (C_2), 130.5 (ArC), 129.6, 122.2, 117.1, 115.5, 102.9 (C_3), 70.5 (C_6), 50.5 (C_7), 44.9 (C_5), 44.0 (C_4), 21.8 ($CO\underline{C}H_3$). HRMS (ESI) calcd for $C_{17}H_{19}F_3N_3O_6$ $[M + CF_3COO]^-$, 418.1231; found, 418.1235.

Methyl 5-Acetamido-2,6-anhydro-3,5-dideoxy-6-formyl-L-*gluco*-hex-2-enonate (7). Aldehyde **7** was prepared according to known protocols.[43] The compound was typically isolated as a mixture of the aldehyde and the methanolic hemiacetal. ^1H NMR (500 MHz, CD_3OD) δ 8.19−8.13 (m, 1H, COOH), 6.02−5.97 (m, 1H, H-3), 4.72−4.69 (m, 1H, H-7), 4.39−4.00 (m, 3H, H-4, H-6, H-5), 4.01−3.78 (m, 3H, $COOCH_3$), 1.96−1.92 (m, 3H, CH_3). ^{13}C NMR (125 MHz, CD_3OD) δ 172.4−171.7 ($\underline{C}OCH_3$), 163.1−160.4 ($\underline{C}OOH$), 145.2−142.8 (C_2), 111.7−105.6 (C_3), 95.6−94.3 (C_7), 78.7−78.5 (C_5), 66.5−64.5 (C_4), 51.7−51.4 ($COO\underline{C}H_3$), 49.7−49.4 (C_6), 21.3-21.1 ($CO\underline{C}H_3$). HRMS (ESI) calcd for the methanolic hemiacetal sodium adduct, $C_{11}H_{17}NNaO_7$ $[M + Na]^+$, 298.0897; found, 298.0896.

5-Acetamido-2,6-anhydro-3,5-dideoxy-6-((phenylamino)-methyl)-L-*gluco*-hex-2-enonic Acid (8a). Compound **8a** was prepared by coupling of compound **7** and aniline following the general procedure given above. The product was obtained in three steps and 74% yield. ^1H NMR (500 MHz, D_2O) δ 7.59−7.56 (m, 3H, ArH), 7.55−7.51 (m, 2H, ArH), 6.24−6.24 (d, J = 4.5 Hz, 1H, H-3), 4.30−4.28 (m, 1H, H-6), 4.10 (s, 1H, H-5), 4.09−4.07 (dd, J = 4.5, 2.0 Hz, 1H, H-4), 3.75−3.74 (m, 2H, H-7), 1.98 (s, 3H, CH_3). ^{13}C NMR (125 MHz, D_2O) δ 175.3 ($\underline{C}OCH_3$), 166.5 ($\underline{C}OOH$), 163.9 (ArC_1), 145.9 (C_2), 131.4 (ArC_3), 131.0 (ArC_2), 123.4 (ArC_4), 110.3 (C_3), 69.8 (C_6), 63.2 (C_4), 52.5 (C_7), 49.8 (C_5), 22.5 ($CO\underline{C}H_3$). HRMS (ESI) calcd for $C_{15}H_{17}N_2O_5$ $[M - H]^-$, 305.1143; found, 305.1144.

5-Acetamido-2,6-anhydro-3,5-dideoxy-6-((benzylamino)-methyl)-L-*gluco*-hex-2-enonic Acid (8b). Compound **8b** was prepared by coupling of compound **7** and benzylamine following the general procedure given above. The product was obtained in three steps and 70% yield. ^1H NMR (500 MHz, D_2O) δ 7.47 (s, 5H, ArH), 6.25−6.23 (d, J = 5.5 Hz, 1H, H-3), 4.38−4.35 (dd, J = 8.5, 4.0 Hz, 1H, H-6), 4.30 (s, 2H, CH_2), 4.10 (s, 1H, H-5), 4.07−4.06 (d, J = 5.5 Hz, H-4), 3.36−3.34 (m, 2H, H-7), 1.94 (s, 3H, CH_3). ^{13}C NMR (125 MHz, D_2O) δ 174.5 ($\underline{C}OCH_3$), 165.2 ($\underline{C}OOH$), 144.5 (ArC_1), 130.3 (C_2), 130.0 (ArC_3), 129.8 (ArC_2), 129.3 (ArC_4), 109.8 (C_3), 69.8 (C_6), 62.2 (C_4), 51.4 ($\underline{C}H_2Ph$), 49.0 (C_5), 47.5 (C_7), 21.6 ($CO\underline{C}H_3$). HRMS (ESI) calcd for $C_{16}H_{21}N_2O_5$ $[M + H]^+$, 321.1445; found, 321.1439.

5-Acetamido-2,6-anhydro-3,5-dideoxy-6-((2-([1,1′-biphenyl]-4-ylmethyl)hydrazinyl)methyl)-L-*gluco*-hex-2-enonic Acid (8c). Compound **8c** was prepared by coupling of compound **7** and ([1,1′-biphenyl]-4-ylmethyl)hydrazine following the general procedure given above. The product was obtained in three steps in 42% yield. ^1H NMR (600 MHz, D_2O) δ 7.75−7.71 (m, 4H, ArH), 7.58−7.52 (m, 4H, ArH), 7.46−7.43 (m, 1H, ArH), 5.99−5.98 (d, J = 2.0 Hz, 1H, H-3), 4.41−4.31 (m, 3H, H-4, CH_2), 4.20−4.20 (m, 1H, H-6), 3.95−3.92 (t, J = 7.5 Hz, 1H, H-5), 3.33−3.32 (m, 2H, H-7), 2.02 (s, 3H, CH_3). ^{13}C NMR (125 MHz, CD_3OD) δ 172.0 ($\underline{C}OCH_3$), 168.5 ($\underline{C}OOH$), 148.5 (C_2), 140.9 (ArC), 139.8 (ArC), 137.8 (ArC), 129.5 (ArC), 128.3 (ArC), 126.7 (ArC), 126.5 (ArC), 126.3 (ArC), 106.7 (C_3), 75.5 (C_6), 66.8 (C_4), 60.0 ($\underline{C}H_2Ph$), 52.3 (C_5), 50.3 (C_7), 21.4 ($CO\underline{C}H_3$). HRMS (ESI) calcd for $C_{22}H_{26}N_3O_5$ $[M + H]^+$, 412.1867; found, 412.1867.

General Protocol for Inhibition Assays. NEU3 and NEU2 were expressed in *E. coli* as N-terminal MBP fusion proteins and purified as described previously.[50] NEU4 was expressed as a GST fusion protein and purified as described.[51] NEU1 was purified as previously described.[48] Assays were conducted in 0.1 M sodium acetate buffer at the enzyme optimum pH (pH 4.5 for NEU1, NEU3, and NEU4; pH 5.5 for NEU2), using a similar amount of enzymatic activity for all four proteins, as determined by assay with 4MU-NANA. Inhibitors were subjected to 3-fold serial dilutions starting from a final concentration of 1 mM. Dilutions were performed in reaction buffer (20 μL). The mixture was then incubated for 15 min at 37 °C. Fluorogenic substrate (4MU-NANA, 50 μM final concentration) was added to the reaction buffer (20 μL) and incubated at 37 °C for 30 min. The reaction was quenched with 200 μL of 0.2 M sodium glycinate buffer, pH 10.7, and enzyme activity was determined by measuring fluorescence (λ_{ex} = 365 nm excitation; λ_{em} = 445 nm emission) in a 384-well plate using a plate reader (Molecular Devices, Sunnyvale CA). Assays were performed with four replicates for each point. Error bars indicate the standard deviation. Reported IC_{50} values were determined by nonlinear regression using SigmaPlot 12. For curves that showed less than a 50% decrease in signal, fits were conducted using the maximum inhibition values found for DANA.

K_i Determinations. Solutions of 4MU-NANA in sodium acetate buffer (0.1 M) at the optimum pH of the target enzyme were prepared with concentrations of 20, 40, 60, 80, and 100 μM. Each substrate solution (25 μL) was mixed with an equal volume of a solution containing serial concentrations of the inhibitor and the target enzyme. The inhibitor concentrations were selected as a range that included the determined IC_{50} value. The reaction mixture (50 μL) was transferred to a 384-well plate. The rate of the product formation at 37 °C was followed by measuring the fluorescence (λ_{ex} = 365 nm excitation; λ_{em} = 445 nm emission) every 30 s for 60 min using a plate reader (Molecular Devices, Sunnyvale CA). Pseudo-first-order rates were determined using the initial linear part of the resulting curves. The double reciprocal plot (1/rate versus 1/[S]) for each inhibitor concentration was used to determine a slope, and a plot of the slopes versus inhibitor concentration was fit to determine K_i.

Molecular Modeling. The homology model of NEU3 was the same as reported previously.[50] Molecular docking to the protein models was performed using Autodock 4.2 using a 60^3 Å grid centered on the active site with 0.375 Å resolution.[54,55] The 200 lowest energy ligand poses were evaluated by cluster analysis, and the lowest energy conformer that maintained key contacts to the active site was selected as the starting point for further analysis by molecular dynamics calculations. Molecular dynamics were performed using MacroModel 9.9 from an initial protein−ligand complex obtained from docking. The complex was first equilibrated for 100 ps at 300 K, followed by 10

ns dynamics at 300 K with 1.5 fs time steps. The force field used was AMBER* with a GB/SA continuum solvation model.[61] All simulations were observed to converge (see Supporting Information). The converged structure was then subjected to unconstrained minimization, providing the final model of the protein−ligand complex. Models were visualized in PyMOL,[62] and protein surfaces were calculated using DelPhi.[63]

■ ASSOCIATED CONTENT

Supporting Information

^{1}H and ^{13}C NMR data, HRMS spectra, and HPLC traces for all tested compounds, SDS−PAGE of purified human neuraminidases, IC_{50} curves, pH profiles of the human neuraminidases, and K_i determinations. This material is available free of charge via the Internet at http://pubs.acs.org.

Accession Codes

PDB code used: 1VCU, reported by Chavas et al.[52]

■ AUTHOR INFORMATION

Corresponding Author

*Phone: 780 492 0377. Fax: 780 492 8231. E-mail: ccairo@ualberta.ca.

Author Contributions

Y. Zhang synthesized and characterized compounds. A.A. produced NEU2, NEU3, and NEU4, performed molecular modeling, and conducted enzyme assays. Y. Zou developed synthetic methodology. V.S. prepared NEU1. A.V.P. designed experiments and wrote the manuscript. C.W.C. designed experiments and wrote the manuscript. All authors have given approval to the final version of the manuscript.

Notes

The authors declare no competing financial interest.

■ ACKNOWLEDGMENTS

The authors acknowledge the support by a grant from the Natural Sciences and Engineering Research Council (NSERC) and the Alberta Glycomics Centre. Infrastructure support was provided by the Canadian Foundation for Innovation.

■ ABBREVIATIONS USED

NEU, neuraminidase enzyme; hNEU, human neuraminidase enzyme; *vc*NEU, *Vibrio cholera* sialidase; DANA, 2-deoxy-2,3-didehydro-*N*-acetylneuraminic acid; GH, glycosyl hydrolase; GT, glycosyl transferase; SAR, structure−activity relationship; 4MU-NANA, 2′-(4-methylumbelliferyl)-α-D-*N*-acetylneuraminic acid

■ REFERENCES

(1) Varki, A.; Cummings, R. D.; Esko, J. D.; Freeze, H. H.; Stanley, P.; Bertozzi, C. R.; Hart, G. W.; Etzler, M. E. *Essentials of Glycobiology*, 2nd ed.; Cold Spring Harbor Laboratory Press: Cold Spring Harbor, NY, 2009.

(2) Dwek, R. A. Glycobiology: toward understanding the function of sugars. *Chem. Rev.* **1996**, *96*, 683−720.

(3) Culyba, E. K.; Price, J. L.; Hanson, S. R.; Dhar, A.; Wong, C. H.; Gruebele, M.; Powers, E. T.; Kelly, J. W. Protein native-state stabilization by placing aromatic side chains in N-glycosylated reverse turns. *Science* **2011**, *331*, 571−575.

(4) Tauber, R.; Park, C. S.; Becker, A.; Geyer, R.; Reutter, W. Rapid intramolecular turnover of N-linked glycans in plasma membrane glycoproteins—extension of intramolecular turnover to the core sugars in plasma membrane glycoproteins of hepatoma. *Eur. J. Biochem.* **1989**, *186*, 55−62.

(5) Tauber, R.; Park, C. S.; Reutter, W. Intramolecular heterogeneity of degradation in plasma membrane glycoproteins—evidence for a general characteristic. *Proc. Natl. Acad. Sci. U.S.A.* **1983**, *80*, 4026−4029.

(6) Parker, R. B.; Kohler, J. J. Regulation of intracellular signaling by extracellular glycan remodeling. *ACS Chem. Biol.* **2010**, *5*, 35−46.

(7) Pshezhetsky, A. V.; Hinek, A. Where catabolism meets signalling: neuraminidase 1 as a modulator of cell receptors. *Glycoconjugate J.* **2011**, *28*, 441−452.

(8) Gloster, T. M.; Vocadlo, D. J. Developing inhibitors of glycan processing enzymes as tools for enabling glycobiology. *Nat. Chem. Biol.* **2012**, *8*, 683−694.

(9) Goi, G.; Bairati, C.; Massaccesi, L.; Lovagnini, A.; Lombardo, A.; Tettamanti, G. Membrane anchoring and surface distribution of glycohydrolases of human erythrocyte membranes. *FEBS Lett.* **2000**, *473*, 89−94.

(10) Aureli, M.; Masilamani, A. P.; Illuzzi, G.; Loberto, N.; Scandroglio, F.; Prinetti, A.; Chigorno, V.; Sonnino, S. Activity of plasma membrane beta-galactosidase and beta-glucosidase. *FEBS Lett.* **2009**, *583*, 2469−2473.

(11) Porwoll, S.; Loch, N.; Kannicht, C.; Nuck, R.; Grunow, D.; Reutter, W.; Tauber, R. Cell surface glycoproteins undergo postbiosynthetic modification of their *N*-glycans by stepwise demannosylation. *J. Biol. Chem.* **1998**, *273*, 1075−1085.

(12) Cordero, O. J.; Merino, A.; de la Cadena, M. P.; Bugía, B.; Nogueira, M.; Viñuela, J. E.; Martínez-Zorzano, V. S.; de Carlos, A.; Rodríguez-Berrocal, F. J. Cell surface human alpha-L-fucosidase. *Eur. J. Biochem.* **2001**, *268*, 3321−3331.

(13) Monti, E.; Bonten, E.; D'Azzo, A.; Bresciani, R.; Venerando, B.; Borsani, G.; Schauer, R.; Tettamanti, G. Sialidases in Vertebrates: A Family of Enzymes Tailored for Several Cell Functions. In *Advances in Carbohydrate Chemistry and Biochemistry*, Academic Press: New York, 2010; Vol. *64*, pp 403−479.

(14) Feng, C.; Zhang, L.; Almulki, L.; Faez, S.; Whitford, M.; Hafezi-Moghadam, A.; Cross, A. S. Endogenous PMN sialidase activity exposes activation epitope on CD11b/CD18 which enhances its binding interaction with ICAM-1. *J. Leukocyte Biol.* **2011**, *90*, 313−321.

(15) Stamatos, N. M.; Carubelli, I.; van de Vlekkert, D.; Bonten, E. J.; Papini, N.; Feng, C. G.; Venerando, B.; d'Azzo, A.; Cross, A. S.; Wang, L. X.; Gomatos, P. J. LPS-induced cytokine production in human dendritic cells is regulated by sialidase activity. *J. Leukocyte Biol.* **2010**, *88*, 1227−1239.

(16) Nan, X.; Carubelli, I.; Stamatos, N. M. Sialidase expression in activated human T lymphocytes influences production of IFN-γ. *J. Leukocyte Biol.* **2007**, *81*, 284−296.

(17) Yamaguchi, K.; Shiozaki, K.; Moriya, S.; Koseki, K.; Wada, T.; Tateno, H.; Sato, I.; Asano, M.; Iwakura, Y.; Miyagi, T. Reduced susceptibility to colitis-associated colon carcinogenesis in mice lacking plasma membrane-associated sialidase. *PLoS One* **2012**, *7*, e41132.

(18) Miyagi, T. Mammalian sialidases and their functions. *Trends Glycosci. Glycotechnol.* **2010**, *22*, 162−172.

(19) Miyagi, T.; Yamaguchi, K. Mammalian sialidases: physiological and pathological roles in cellular functions. *Glycobiology* **2012**, *22*, 880−896.

(20) Cherayil, G. D. Sialic acid and fatty acid concentrations in lymphocytes, red blood cells and plasma from patients with multiple sclerosis. *J. Neurol. Sci.* **1984**, *63*, 1−10.

(21) Stelmasiak, Z.; Solski, J.; Jakubowska, B. Sialic acids in serum and erythrocyte membranes in patients with MS. *Neuropsychiatrie* **1996**, *10*, 205−208.

(22) Cantarel, B. L.; Coutinho, P. M.; Rancurel, C.; Bernard, T.; Lombard, V.; Henrissat, B. The carbohydrate-active enzymes database (CAZy): an expert resource for glycogenomics. *Nucleic Acids Res.* **2009**, *37*, D233−D238.

(23) Monti, E.; Preti, A.; Venerando, B.; Borsani, G. Recent development in mammalian sialidase molecular biology. *Neurochem. Res.* **2002**, *27*, 649−663.

(24) Lukong, K. E.; Seyrantepe, V.; Landry, K.; Trudel, S.; Ahmad, A.; Gahl, W. A.; Lefrancois, S.; Morales, C. R.; Pshezhetsky, A. V.

Intracellular distribution of lysosomal sialidase is controlled by the internalization signal in its cytoplasmic tail. *J. Biol. Chem.* **2001**, *276*, 46172−46181.
(25) Vinogradova, M. V.; Michaud, L.; Mezentsev, A. V.; Lukong, K. E.; El-Alfy, M.; Morales, C. R.; Potier, M.; Pshezhetsky, A. V. Molecular mechanism of lysosomal sialidase deficiency in galactosialidosis involves its rapid degradation. *Biochem. J.* **1998**, *330*, 641−650.
(26) Monti, E.; Preti, A.; Rossi, E.; Ballabio, A.; Borsani, G. Cloning and characterization of NEU2, a human gene homologous to rodent soluble sialidases. *Genomics* **1999**, *57*, 137−143.
(27) Miyagi, T.; Tsuiki, S. Purification and characterization of cytosolic sialidase from rat liver. *J. Biol. Chem.* **1985**, *260*, 6710−6716.
(28) Tringali, C.; Papini, N.; Fusi, P.; Croci, G.; Borsani, G.; Preti, A.; Tortora, P.; Tettamanti, G.; Venerando, B.; Monti, E. Properties of recombinant human cytosolic sialidase HsNEU2. The enzyme hydrolyzes monomerically dispersed GM1 ganglioside molecules. *J. Biol. Chem.* **2004**, *279*, 3169−79.
(29) Wang, Y.; Yamaguchi, K.; Wada, T.; Hata, K.; Zhao, X. J.; Fujimoto, T.; Miyagi, T. A close association of the ganglioside-specific sialidase Neu3 with caveolin in membrane microdomains. *J. Biol. Chem.* **2002**, *277*, 26252−26259.
(30) Zanchetti, G.; Colombi, P.; Manzoni, M.; Anastasia, L.; Caimi, L.; Borsani, G.; Venerando, B.; Tettamanti, G.; Preti, A.; Monti, E.; Bresciani, R. Sialidase NEU3 is a peripheral membrane protein localized on the cell surface and in endosomal structures. *Biochem. J.* **2007**, *408*, 211−219.
(31) Yamaguchi, K.; Hata, K.; Koseki, K.; Shiozaki, K.; Akita, H.; Wada, T.; Moriya, S.; Miyagi, T. Evidence for mitochondrial localization of a novel human sialidase (NEU4). *Biochem. J.* **2005**, *390*, 85−93.
(32) Monti, E.; Bassi, M. T.; Bresciani, R.; Civini, S.; Croci, G. L.; Papini, N.; Riboni, M.; Zanchetti, G.; Ballabio, A.; Preti, A.; Tettamanti, G.; Venerando, B.; Borsani, G. Molecular cloning and characterization of NEU4, the fourth member of the human sialidase gene family. *Genomics* **2004**, *83*, 445−453.
(33) Seyrantepe, V.; Landry, K.; Trudel, S.; Hassan, J. A.; Morales, C. R.; Pshezhetsky, A. V. Neu4, a novel human lysosomal lumen sialidase, confers normal phenotype to sialidosis and galactosialidosis cells. *J. Biol. Chem.* **2004**, *279*, 37021−37029.
(34) Seyrantepe, V.; Poupetova, H.; Froissart, R.; Zabot, M. T.; Maire, I.; Pshezhetsky, A. V. Molecular pathology of NEU1 gene in sialidosis. *Hum. Mutat.* **2003**, *22*, 343−352.
(35) Wang, P.; Zhang, J.; Bian, H.; Wu, P.; Kuvelkar, R.; Kung, T. T.; Crawley, Y.; Egan, R. W.; Billah, M. M. Induction of lysosomal and plasma membrane-bound sialidases in human T-cells via T-cell receptor. *Biochem. J.* **2004**, *380*, 425−433.
(36) Sandbhor, M. S.; Soya, N.; Albohy, A.; Zheng, R. B.; Cartmell, J.; Bundle, D. R.; Klassen, J. S.; Cairo, C. W. Substrate recognition of the membrane-associated sialidase NEU3 requires a hydrophobic aglycone. *Biochemistry* **2011**, *50*, 6753−6762.
(37) Li, Y.; Cao, H.; Yu, H.; Chen, Y.; Lau, K.; Qu, J.; Thon, V.; Sugiarto, G.; Chen, X. Identifying selective inhibitors against the human cytosolic sialidase NEU2 by substrate specificity studies. *Mol. BioSyst.* **2011**, *7*, 1060−1072.
(38) Khedri, Z.; Li, Y.; Cao, H.; Qu, J.; Yu, H.; Muthana, M. M.; Chen, X. Synthesis of selective inhibitors against *V. cholerae* sialidase and human cytosolic sialidase NEU2. *Org. Biomol. Chem.* **2012**, *10*, 6112−6120.
(39) Magesh, S.; Moriya, S.; Suzuki, T.; Miyagi, T.; Ishida, H.; Kiso, M. Design, synthesis, and biological evaluation of human sialidase inhibitors. Part 1: Selective inhibitors of lysosomal sialidase (NEU1). *Bioorg. Med. Chem. Lett.* **2008**, *18*, 532−537.
(40) Li, J.; Zheng, M.; Tang, W.; He, P.-L.; Zhu, W.; Li, T.; Zuo, J.-P.; Liu, H.; Jiang, H. Syntheses of triazole-modified zanamivir analogues via click chemistry and anti-AIV activities. *Bioorg. Med. Chem. Lett.* **2006**, *16*, 5009−5013.
(41) von Itzstein, M.; Wu, W.-Y.; Jin, B. The synthesis of 2,3-didehydro-2,4-dideoxy-4-guanidinyl-*N*-acetylneuraminic acid: a potent influenza virus sialidase inhibitor. *Carbohydr. Res.* **1994**, *259*, 301−305.
(42) Lu, Y.; Gervay-Hague, J. Synthesis of C-4 and C-7 triazole analogs of zanamivir as multivalent sialic acid containing scaffolds. *Carbohydr. Res.* **2007**, *342*, 1636−1650.
(43) Meindl, P.; Tuppy, H. 2-Deoxy-2,3-dehydro-sialinsäuren, 3. Mitt.: Hemmung der *Vibrio cholerae*-neuraminidase durch oxidationsprodukte der 2-deoxy-2,3-dehydro-*N*-acetylneuraminsäure. *Monatsh. Chem.* **1970**, *101*, 639−647.
(44) Smith, P. W.; Sollis, S. L.; Howes, P. D.; Cherry, P. C.; Cobley, K. N.; Taylor, H.; Whittington, A. R.; Scicinski, J.; Bethell, R. C.; Taylor, N.; Skarzynski, T.; Cleasby, A.; Singh, O.; Wonacott, A.; Varghese, J.; Colman, P. Novel inhibitors of influenza sialidases related to GG167: structure−activity, crystallographic and molecular dynamic studies with 4*H*-pyran-2-carboxylic acid 6-carboxamides. *Bioorg. Med. Chem. Lett.* **1996**, *6*, 2931−2936.
(45) Smith, P. W.; Sollis, S. L.; Howes, P. D.; Cherry, P. C.; Starkey, I. D.; Cobley, K. N.; Weston, H.; Scicinski, J.; Merritt, A.; Whittington, A.; Wyatt, P.; Taylor, N.; Green, D.; Bethell, R.; Madar, S.; Fenton, R. J.; Morley, P. J.; Pateman, T.; Beresford, A. Dihydropyrancarboxamides related to zanamivir: a new series of inhibitors of influenza virus sialidases. 1. Discovery, synthesis, biological activity, and structure−activity relationships of 4-guanidino- and 4-amino-4*H*-pyran-6-carboxamides. *J. Med. Chem.* **1998**, *41*, 787−797.
(46) Sollis, S. L.; Smith, P. W.; Howes, P. D.; Cherry, P. C.; Bethell, R. C. Novel inhibitors of influenza sialidase related to GG167 synthesis of 4-amino and guanidino-4*H*-pyran-2-carboxylic acid-6-propylamides. Selective inhibitors of influenza A virus sialidase. *Bioorg. Med. Chem. Lett.* **1996**, *6*, 1805−1808.
(47) Politzer, P.; Murray, J. S. Some Intrinsic Features of Hydroxylamines, Oximes and Hydroxamic Acids: Integration of Theory and Experiment. In *The Chemistry of Hydroxylamines, Oximes and Hydroxamic Acids*; John Wiley & Sons, Ltd.: Chichester, U.K., 2008; pp 1−27.
(48) Pshezhetsky, A. V.; Potier, M. Association of *N*-acetylgalactosamine-6-sulfate sulfatase with the multienzyme lysosomal complex of *β*-galactosidase, cathepsin A, and neuraminidase. *J. Biol. Chem.* **1996**, *271*, 28359−28365.
(49) Watson, D. C.; Leclerc, S.; Wakarchuk, W. W.; Young, N. M. Enzymatic synthesis and properties of glycoconjugates with legionaminic acid as a replacement for neuraminic acid. *Glycobiology* **2010**, *21*, 99−108.
(50) Albohy, A.; Li, M. D.; Zheng, R. B.; Zou, C.; Cairo, C. W. Insight into substrate recognition and catalysis by the mammalian neuraminidase 3 (NEU3) through molecular modeling and site directed mutagenesis. *Glycobiology* **2010**, *20*, 1127−1138.
(51) Albohy, A.; Mohan, S.; Zheng, R. B.; Pinto, B. M.; Cairo, C. W. Inhibitor selectivity of a new class of oseltamivir analogs against viral neuraminidase over human neuraminidase enzymes. *Bioorg. Med. Chem.* **2011**, *19*, 2817−22.
(52) Chavas, L. M. G.; Tringali, C.; Fusi, P.; Venerando, B.; Tettamanti, G.; Kato, R.; Monti, E.; Wakatsuki, S. Crystal structure of the human cytosolic sialidase Neu2—evidence for the dynamic nature of substrate recognition. *J. Biol. Chem.* **2005**, *280*, 469−475.
(53) Zou, Y.; Albohy, A.; Sandbhor, M.; Cairo, C. W. Inhibition of human neuraminidase 3 (NEU3) by *C*9-triazole derivatives of 2,3-didehydro-*N*-acetyl-neuraminic acid. *Bioorg. Med. Chem. Lett.* **2010**, *20*, 7529−7533.
(54) Goodsell, D. S.; Morris, G. M.; Olson, A. J. Automated docking of flexible ligands: applications of AutoDock. *J. Mol. Recognit.* **1996**, *9*, 1−5.
(55) Morris, G. M.; Goodsell, D. S.; Halliday, R. S.; Huey, R.; Hart, W. E.; Belew, R. K.; Olson, A. J. Automated docking using a Lamarckian genetic algorithm and an empirical binding free energy function. *J. Comput. Chem.* **1998**, *19*, 1639−1662.
(56) von Itzstein, M. The war against influenza: discovery and development of sialidase inhibitors. *Nat. Rev. Drug Discovery* **2007**, *6*, 967−974.
(57) Hata, K.; Koseki, K.; Yamaguchi, K.; Moriya, S.; Suzuki, Y.; Yingsakmongkon, S.; Hirai, G.; Sodeoka, M.; Von Itzstein, M.; Miyagi,

T. Limited inhibitory effects of oseltamivir and zanamivir on human sialidases. *Antimicrob. Agents Chemother.* **2008**, *52*, 3484−3491.
(58) Chavas, L. M. G.; Kato, R.; Suzuki, N.; von Itzstein, M.; Mann, M. C.; Thomson, R. J.; Dyason, J. C.; McKimm-Breschkin, J.; Fusi, P.; Tringali, C.; Venerando, B.; Tettamanti, G.; Monti, E.; Wakatsuki, S. Complexity in influenza virus targeted drug design: interaction with human sialidases. *J. Med. Chem.* **2010**, *53*, 2998−3002.
(59) Magesh, S.; Suzuki, T.; Miyagi, T.; Ishida, H.; Kiso, M. Homology modeling of human sialidase enzymes NEU1, NEU3 and NEU4 based on the crystal structure of NEU2: hints for the design of selective NEU3 inhibitors. *J. Mol. Graphics Modell.* **2006**, *25*, 196−207.
(60) Bashiardes, G.; Bodwell, G. J.; Davies, S. G. Asymmetric synthesis of (−)-actinonin and (−)-epi-actinonin. *J. Chem. Soc., Perkin Trans. 1* **1993**, 459−469.
(61) Still, W. C.; Tempczyk, A.; Hawley, R. C.; Hendrickson, T. Semianalytical treatment of solvation for molecular mechanics and dynamics. *J. Am. Chem. Soc.* **1990**, *112*, 6127−6129.
(62) *The PyMOL Molecular Graphics System*, version 1.5.0.4; Schrodinger, LLC: New York; http://www.pymol.org/ (accessed November 15, 2012).
(63) Gilson, M. K.; Sharp, K. A.; Honig, B. H. Calculating the electrostatic potential of molecules in solution: method and error assessment. *J. Comput. Chem.* **1988**, *9*, 327−335.